

KAWASAKI STEEL TECHNICAL REPORT

No.2 (March 1981)

Manufacture of Forgings for Nuclear Pressure Vessel

Hiroshige Wanaka, Kazuo Asoh, Katsuhiko Miyata, Tatsuhiko Kato, Toru Saito, Akira Horiuchi, Susumu Matsui, Shingo Sato, Michihiro Tanaka

Synopsis :

Experimental manufacture has been performed of a top head flange and a monoblock bottom head dome for the BWR 800-MWe class nuclear pressure vessel. The top head flange was forged from a 165 t ingot made from a two-heat-mixture of BOG-LRF and BOF-EF-LRF melts. The bottom head dome was forged from a 115 t ingot by the BOF-LRF process and was press-formed using a spherical upper mold and a ring-shaped lower mold. Deformation of the bottom head dome was performed very uniformly and no scale defects occurred during forming. In spite of the largeness of the ingot used, both products showed uniform distributions of chemical composition and mechanical properties, thus suggesting their suitable application for a nuclear pressure vessel. Examinations have revealed the high quality of these forgings in relation to internal qualities, tensile properties, fracture toughness, fatigue properties and others.

(c)JFE Steel Corporation, 2003

<p>The body can be viewed from the next page.</p>

Manufacture of Forgings for Nuclear Pressure Vessel*

Hiroshige WANAKA **

Tatsuhiko KATO **

Susumu MATSUI ***

Kazuo ASOH **

Toru SAITO **

Shingo SATO ***

Katsuhiko MIYATA **

Akira HORIUCHI **

Michihiro TANAKA ***

Experimental manufacture has been performed of a top head flange and a monoblock bottom head dome for the BWR 800-MWe class nuclear pressure vessel. The top head flange was forged from a 165 t ingot made from a two-heat-mixture of BOF-LRF and BOF-EF-LRF melts. The bottom head dome was forged from a 115 t ingot by the BOF-LRF process and was press-formed using a spherical upper mold and a ring-shaped lower mold. Deformation of the bottom head dome was performed very uniformly and no scale defects occurred during forming. In spite of the largeness of the ingot used, both products showed uniform distributions of chemical composition and mechanical properties, thus suggesting their suitable application for a nuclear pressure vessel. Examinations have revealed the high quality of these forgings in relation to internal qualities, tensile properties, fracture toughness, fatigue properties and others.

1 Introduction

Power-generating nuclear reactors which are in operation in Japan mainly consist of boiling water reactors (BWRs) and pressurized water reactors (PWRs)—the so-called “light water reactors.” The light water reactor is broadly composed of the reactor core construction, pressure vessel, storing vessel, piping and heat-exchangers; and the percentage of forgings in relation to all the units of the reactor is increasing, owing to their quality and reliability. Particularly for materials to be used for the pressure vessel, the need for soundness and reliability has become increasingly severe; and along with the trend of an increasingly enlarging size of the pressure vessel, raw material manufacturers are now required to establish production techniques that can cope with such requirements and to provide a stringent quality control system.

Manufacture of forgings for the pressure vessel at Mizushima Works of our company was undertaken on a full scale, following the installation of large-sized forging equipment¹⁻³⁾ including the ladle refining furnace (LRF) introduced from ASEA-SKF and the 6 000 t free forging press imported from HYDRAULIK of West Germany. Trial manufacture and property

verification⁴⁾ of raw materials for the 524-MWe class SA 508 C1.2 top head flange and nozzles were soon completed, and continuous studies have been conducted on how to improve their quality and performance. On the other hand, the Works' quality control system⁵⁾ was established through acquisition of the Quality System Certificate according to the ASME Boiler and Pressure Vessel Code Sec. III for thick steel plates and forgings in March, 1977.

With this background, the Works recently accomplished trial manufacture and property verification test of materials for the BWR 800-MWe class JIS SFVV 3 top head flange and the seamless monoblock forged dome (hereinafter called “bottom head dome”), and the results of the test are reported below.

2 Preliminary Examination

Prior to trial manufacture and property verification, examination was made on the target chemical composition of the forgings for the top head flange and bottom head dome and on the flexural forming process of the bottom head dome forgings.

2.1 Targeted Chemical Composition

JIS SFVV 3 steel which is used as forgings for the nuclear pressure vessel is required to have sufficient strength and excellent toughness. Properties required of JIS SFVV 3 steel and some other target properties are shown in Table 1. Namely, it has been stipulated

* Originally published in *Kawasaki Steel Technical Report*, 12 (1980) 1, pp. 52-64 (in Japanese)

** Mizushima Works

*** Research Laboratories

Table 1 Required properties for JIS SFVV3 steel

(a) Chemical composition									(wt.%)
C	Si	Mn	P	S	Ni	Mo	V	ΔG^*	
0.15 ~0.25	0.15 ~0.35	1.20 ~1.50	Max 0.025	Max 0.025	0.40 ~0.80	0.45 ~0.60	Max 0.05	< 0	
$\Delta G = Cr(\%) + 3.3Mo(\%) + 8.1V(\%) - 2$									
(b) Mechanical properties									
Tensile test at room temperature				Impact test		T.S.** at 150 or 200°C (kgf/mm ²)			
Y.S. (kgf/mm ²)	T.S. (kgf/mm ²)	El. (%)	R.A. (%)	VE _{4.4} (kgf/mm ²)	RT ^{**} _{NDT} (°C)				
Min 35	Min 56	Min 18	Min 38	Av.: 4.1min. Min: 3.5min.	Max -30	Min 55			
**Preferable properties not specified in JIS SFV3									

**Preferable properties not specified in JIS SFVV3

that tensile strength at elevated temperatures be 55 kgf/mm² minimum at 150°C and 200°C, and the reference nil-ductility transition temperature (RT_{NDT}) be -30°C maximum. **Fig. 1** shows the relationship between tensile strengths at elevated and room temperatures of this type of steel. In order to achieve a tensile strength of 55 kgf/mm² minimum at temperatures of 150°C and 200°C, it is necessary to obtain a tensile strength of 62 kgf/mm² minimum at room temperature. Regarding the relationship between T.S. at room temperature and toughness, several reports⁶⁻¹⁰⁾ have been made. These reports indicate that the range within which chemical composition can be manipulated is narrow. An increase in the C content will effectively increase the strength, but it will also raise the transition temperature. It is necessary, therefore, to keep the C content at a minimum value within which necessary strength can be maintained according to the plate thickness. **Fig. 2** shows the effect of the cooling rate on strength and toughness of SFVV3 steel of 0.18% and 0.21% C content. Assuming that the plate thickness at heat treatment of the top head flange material and that of the bottom head dome material are about 400 mm and 200 mm, respectively, it can be inferred from **Fig. 2** that a C content of 0.21% is required for the top head flange material which has greater plate thickness, in order to maintain T.S. at room temperature of 62 kgf/mm² minimum. For the bottom head dome material which is thinner, 0.20% C content has been adopted as the target. As for toughness, priority is given to maintaining proper value of T.S. at elevated temperature since toughness will not vary greatly within the range of 0.18% to 0.21% C content. **Table 2** shows the target values of chemical composition of the top head flange and bottom head dome together with their ladle analysis values. In setting the target values,

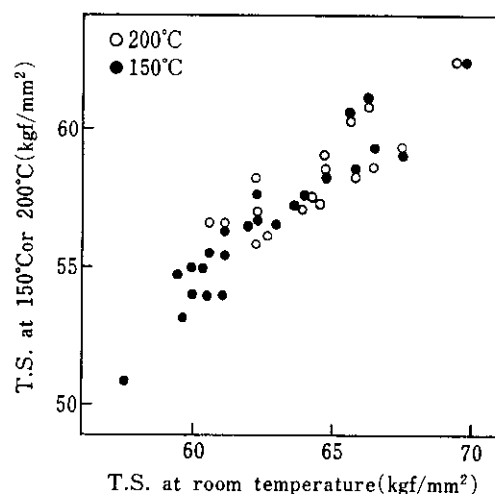


Fig. 1 Comparison of tensile strength at elevated vs. room temperatures

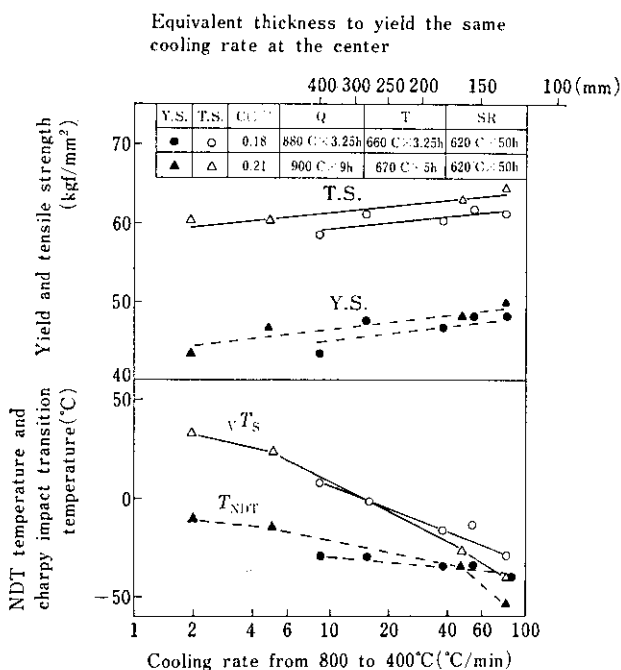


Fig. 2 Effect of cooling rate on strength and toughness of SFVV3 steel

impurity elements such as P and S have been reduced to the minimum and reheating cracking index ΔG ($= \times Cr(\%) + 3.3 Mo(\%) + 8.1 V(\%) - 2$) has been made negative.

2.2 Flexural Forming Process

In order to establish basic techniques for flexural forming, experiments have been conducted with 1/10-scale and full-size models, and examination has

Table 2 Chemical composition of top head flange and bottom head dome

		C	Si	Mn	P	S	Ni	Cr	Mo	Al	N	H
Aimed value		0.20 ~0.22	0.15 ~0.30	1.40 ~1.50	Max 0.008	Max 0.003	0.70 ~0.80	0.10 ~0.14	0.50 ~0.54	0.010 ~0.020	0.0080 ~0.0100	Max 1.5(ppm)
Ladle analysis	Flange	0.21	0.26	1.45	0.006	0.002	0.75	0.12	0.52	0.019	—	1.5(ppm)
	Dome	0.21	0.27	1.44	0.004	0.002	0.75	0.14	0.51	0.020	0.0086	1.4(ppm)

		Cu	Nb	V	Co	B	As	Sb	Sn	Ti	ΔG^*
Aimed value		Max 0.02	Max 0.005	Max 0.007	Max 0.005	Max 0.0003	Max 0.004	Max 0.0005	Max 0.002	Max 0.005	< 0
Ladle analysis	Flange	0.01	<0.001	0.003	0.005	<0.0001	0.002	0.0003	<0.001	0.001	-0.140
	Dome	0.01	<0.001	0.005	0.0046	<0.0001	0.001	0.0003	<0.001	0.001	-0.137

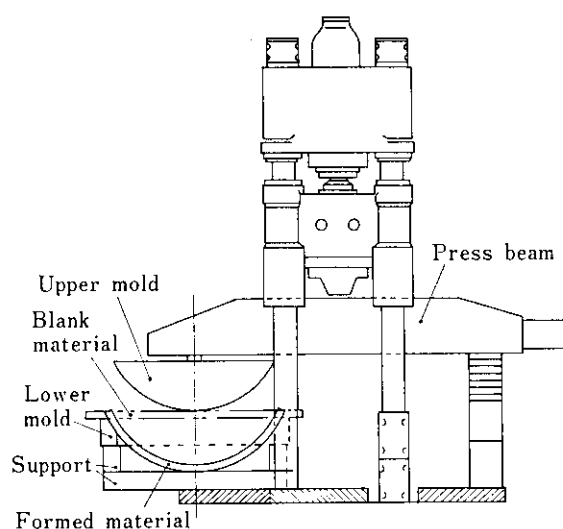
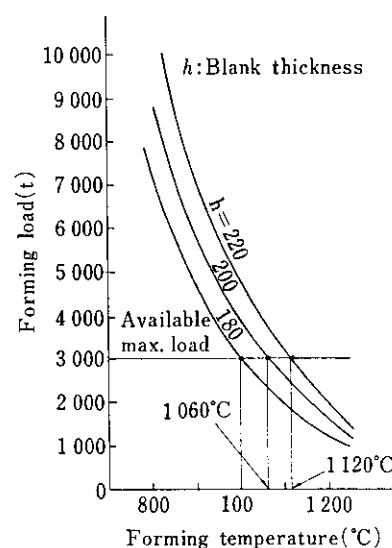
$$\bullet G = Cr(\%) + 3.3Mo(\%) + 8.1V(\%) - 2$$

been made regarding how to obtain a forming method which is most effective in ensuring excellent formability and uniformity of products. In general, possible combinations of upper and lower molds that can be used for forming the dome material are as follows:

- (1) Spherical types for both upper and lower molds
- (2) Spherical type for the upper mold and ring type for the lower mold
- (3) Partial type for the upper mold and spherical type for the lower mold
- (4) Partial types for both upper and lower molds

Out of the above, (3) and (4) are used for partial forming. In flexural forming, deformation shall be uniform and free of partial uneven thickness, while scale scar prevention during forming is important. With these conditions in mind, examination has been

made to select either (1) or (2). First it has been found from the results of the test with the 1/10-scale model that the forming accuracy of the product is highest when the upper mold is made into the spherical type, and is determined by the shape of the upper mold; and thus it has been decided to employ method (2). Next, calculation formulas to be mentioned in 5.2 are used to estimate the forming load that is required for forming the actual product, and test forming with a full-size model has been conducted to determine the optimum conditions including forming load, forming temperature and the forming method. The flexural forming process is shown in Fig. 3, and the relationship between forming load and forming temperature is shown in Fig. 4. The temperature at the

**Fig. 3** Forming assembly for bottom head dome**Fig. 4** Required forming load calculated as a function of forming temperatures and blank thickness for a real size model

time of forming necessary for the maximum screw-down force of 3 000 t used in this method by the 6 000 t press is 1 000°C to 1 150°C. Further, in the flexural forming process, there are problems of plate-thickness variation and rigidity during transportation besides the above-mentioned forming temperature and forming load, and it has been decided to carry out forming by dividing it into three stages.

3 Manufacture of Materials for Top Head Flange and Bottom Head Dome

3.1 Manufacturing Steps

Forgings to be used for the nuclear pressure vessel

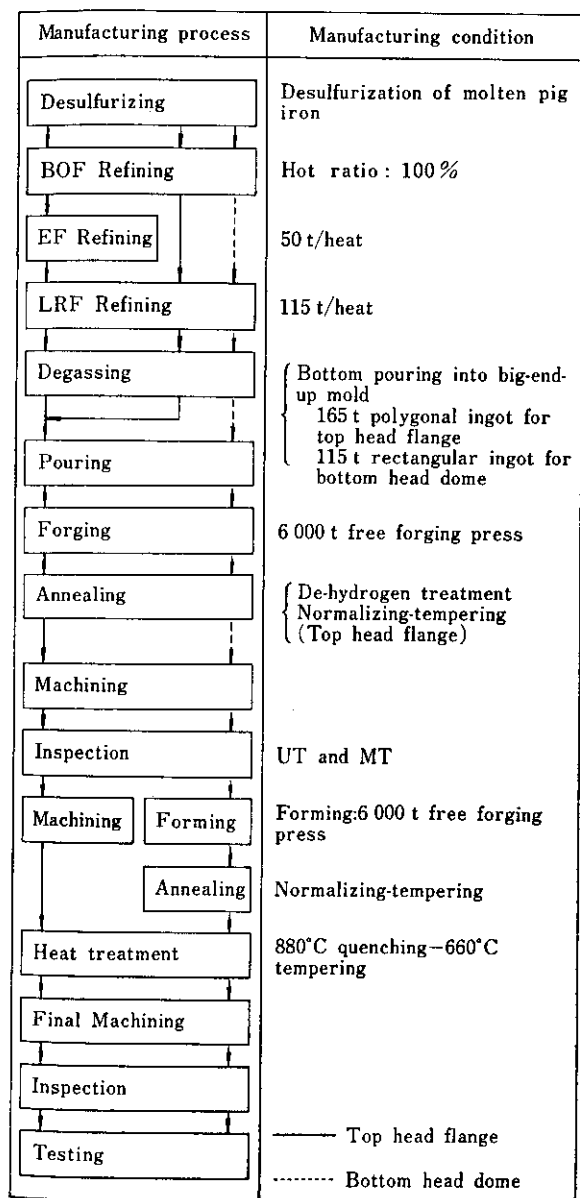


Fig. 5 Manufacturing process of top head flange and bottom head dome

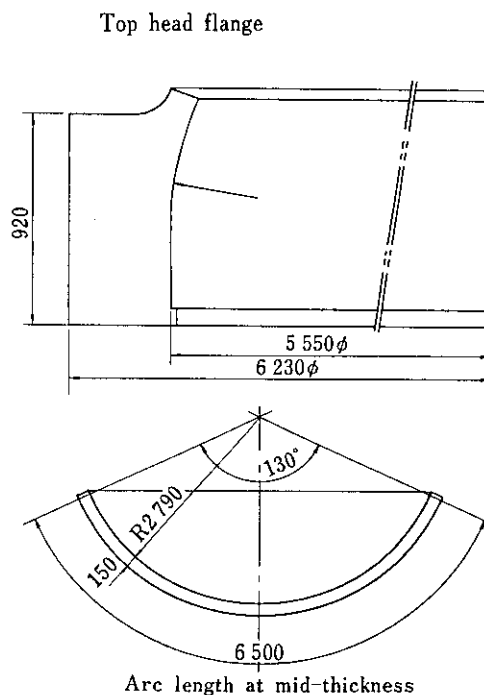


Fig. 6 Dimensions of trial forging for 800 MWe class flange and dome

are required to be of high quality which ensures excellent mechanical properties and highly uniform and free of internal defects. It is no exaggeration to say that most of the internal quality of steel is determined by the steel-making process, and thus we have used our unique LD-LRF process which is most suitable for melting nuclear pressure vessel forging materials. Fig. 5 shows the manufacturing steps and control points for the top head flange and bottom head dome forgings. Fig. 6 shows the dimensions of trial forgings.

3.2 Steelmaking

In making the top head flange material, steel melts by the BOF-LRF process and by the BOF-electric furnace-LRF process were combined and bottom-poured into the big-end-up mold to make a 165 t polygonal ingot, and the bottom head dome material was produced by bottom-pouring the steel melt made by the BOF-LRF process into the big-end-up mold to make a 115 t rectangular ingot. The analysis values of the respective steel melts have already been shown in Table 2. Further, P and S contents were reduced to improve the toughness, and Cu, V, Nb and Ti were also reduced as a measure to cope with embrittlement by neutron irradiation. Contents of these impurities were able to be made very low by executing 100% molten pig iron operation without using scraps.

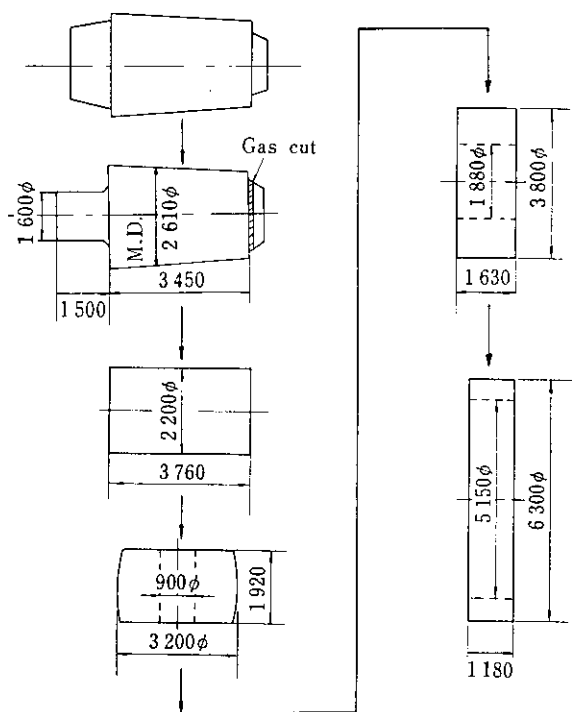


Fig. 7 Forging process of top head flange



Photo. 1 Forging of top head flange

3.3 Forging

Forging was conducted by using the 6 000 t press. The outline of the forging process is shown in Figs. 7 and 8, and the forging condition of the top head flange material is shown in Photo. 1.

3.4 Flexural Forming

As mentioned in the "Preliminary Examination", flexural forming of the bottom head dome material was divided into three stages. The example of the results of dimensional measurements after flexural forming and heat treatment are shown in Fig. 9. It indicates that variation in plate thickness around the same circumference is uniform and forming has

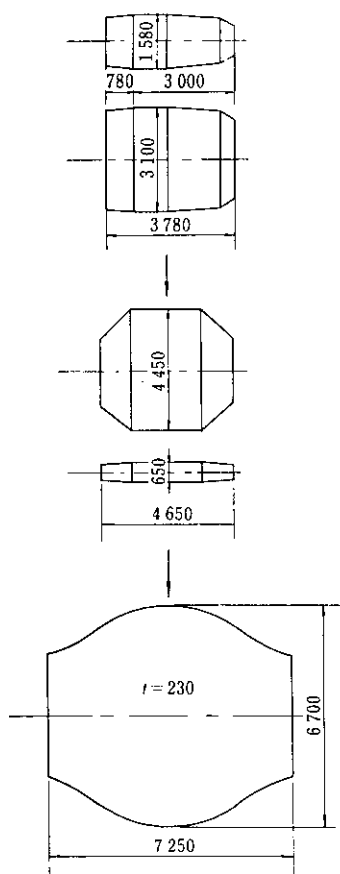


Fig. 8 Forging process of bottom head dome

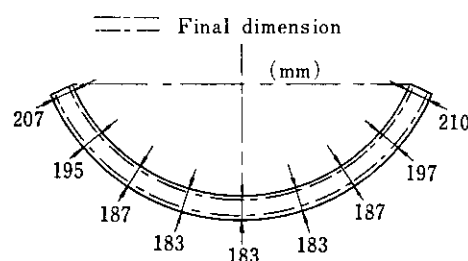


Fig. 9 Dimension of bottom head dome formed and quench-tempered

been carried out smoothly. Also there was little generation of scaling, because forming at each stage was completed in a short period.

3.5 Heat Treatment

Quench-tempering was performed to secure strength and toughness. The quenching temperature was set at 880°C, the tempering temperature at 660°C, and holding time at 0.5 h/in minimum. In order to check the uniformity of temperature and the cooling rate which were the most important control items during heat treatment, thermocouples were fitted at various positions to measure the temperature distribution and its variation. As a representative example, the measuring positions of cooling rate and cooling rates of the bottom head dome material are shown in Table 3. From this table it can be judged that the difference

in cooling rate between measuring positions is small, and heat treatment has been conducted uniformly.

3.6 Inspection at Completion

Dimensional inspection, ultrasonic test and magnetic particle test were conducted. Both the top head flange and bottom head dome forgings revealed no flaws.

4 Results of Property Verification Tests

Base metal fundamental test, fracture toughness test and fatigue test were conducted. Sampling positions at the top head flange and bottom head dome forgings are shown in Fig. 10. The top head flange was sampled at eight positions around the circumference.

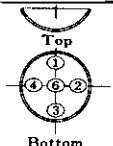
4.1 Chemical Analysis of Products

Results of product analysis for main composition (C, Mn, P, and S) according to JIS G 3212 are shown in Figs. 11 and 12. Segregation is very small to result in a uniform distribution. The results of product analysis also show a good agreement with those of steel heat analysis given in Table 2.

4.2 Internal Properties

In order to evaluate the internal properties of forged steel in a large ingot, tests were carried out on the cleanliness, austenite grain sizes, sulphur prints

Table 3 Cooling rate from 800 to 400°C within bottom head dome

T.C. No.	Through-thickness location			Position and No. of T.C. (Thermo Couple)
	$\frac{1}{4}t$	$\frac{1}{2}t$	$\frac{3}{4}t$	
①	51	31	39	
⑥	51	37	—	
②	56	31	40	
③	43	32	32	
④	61	33	47	

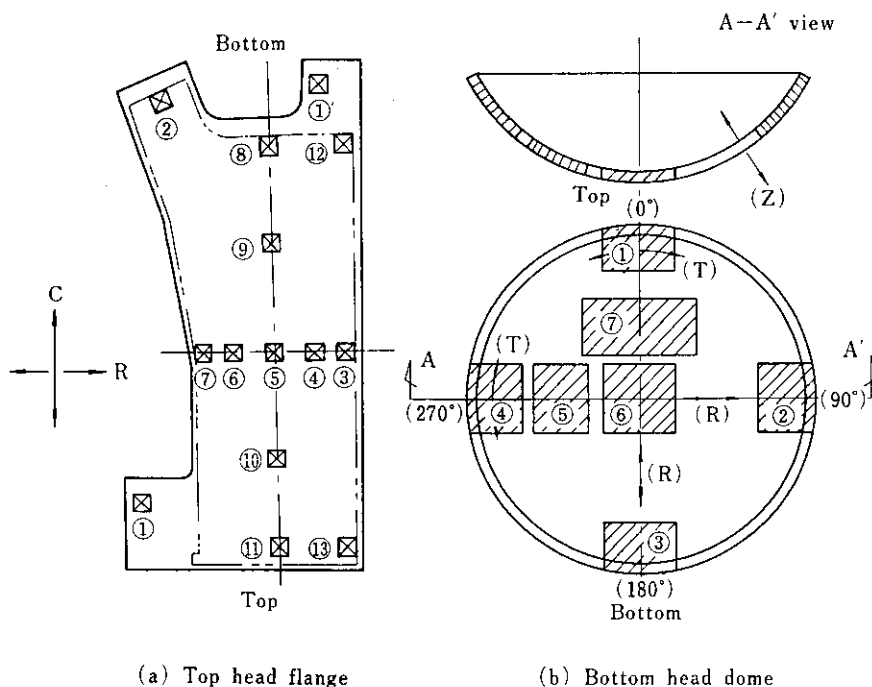


Fig. 10 Sampling positions from forged products

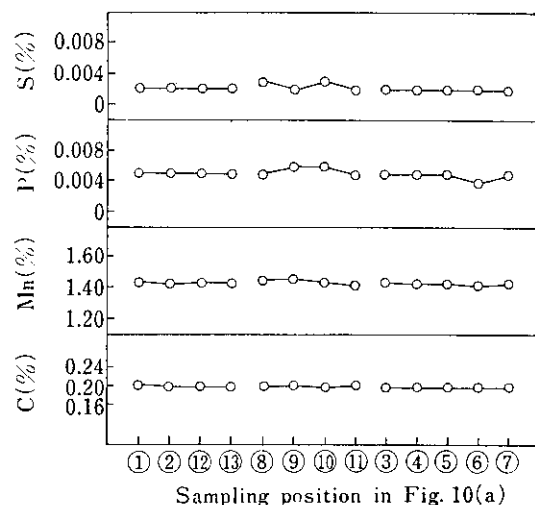


Fig. 11 Distribution of chemical composition in top head flange

and macro- and microstructures. An example of cleanliness of the top head flange measured according to JIS G 0555 is shown in **Table 4**. Non-metallic inclusions are very rare and only A type inclusions are observed here and there. Austenite grain sizes in the top head flange and bottom head dome measured according to JIS G 0551 were fine (Grain Size No.8) at all sampling positions. Microstructures consisted of very fine tempered bainite structures at every sampl-

Table 4 Cleanliness, $d_{60 \times 400}$ by JIS G 0555, of top head flange

(%)				
Position*	dA	dB	dC	d
①	0.017	0.000	0.000	0.017
②	0.017	0.000	0.000	0.017
③	0.021	0.000	0.000	0.021
④	0.013	0.000	0.000	0.013
⑤	0.021	0.000	0.000	0.021
⑥	0.013	0.000	0.000	0.013
⑦	0.013	0.000	0.000	0.013
⑧	0.017	0.000	0.000	0.017
⑨	0.021	0.000	0.000	0.021
⑩	0.008	0.000	0.000	0.008
⑪	0.017	0.000	0.000	0.017
⑫	0.021	0.000	0.000	0.021
⑬	0.021	0.000	0.000	0.021

* Refer to Fig. 10(a) for sampling positions

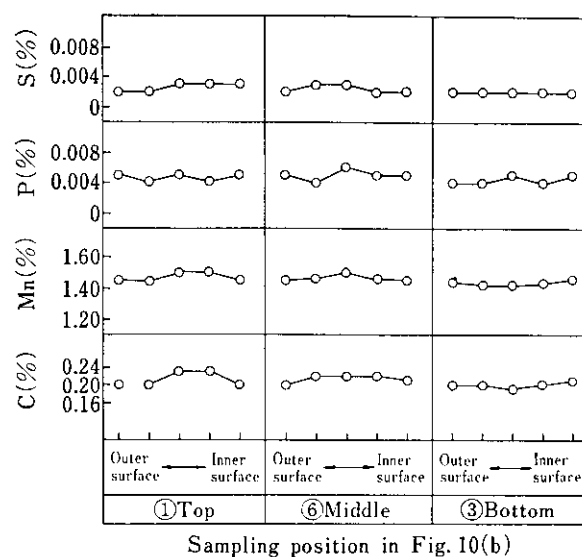


Fig. 12 Through-thickness distribution of chemical composition in bottom head dome

ing position. Austenite grain sizes and microstructures at typical sampling positions are shown in **Photos. 2** and **3**, respectively. The sulphur print test was conducted according to JIS G 0560, and all the sampling positions showed properties of WES Class 1 or above. Also, in the macrostructure test executed according to JIS G 0553, no abnormal segregation was observed. A typical macrostructure of the top head flange is shown in **Photo. 4**. As mentioned above, excellent internal properties were shown in every test, and superiority of forgings produced by the BOF-LRF process was proven.

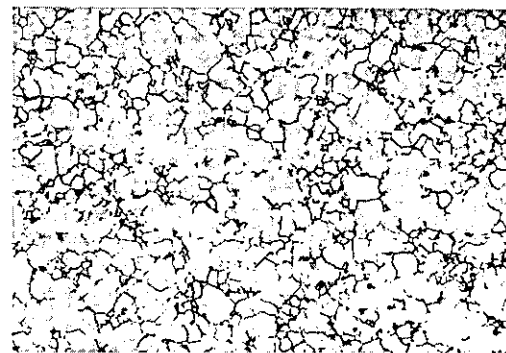
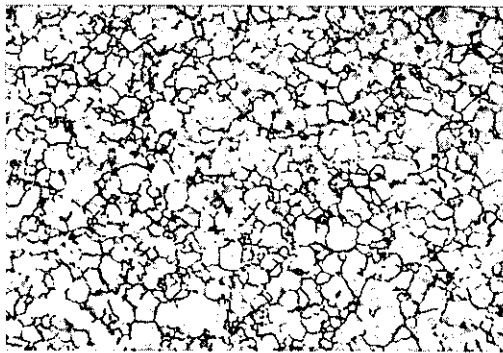
4.3 Tensile Test

Typical examples of the results of the room-temperature tensile test on the top head flange and bottom head dome are shown in **Figs. 13** and **14**, respectively. The difference in strength between the surface layer portion and the central portion was practically nil, and even at the central portion, the originally target tensile strength of 62 kgf/mm² minimum was achieved. In addition, an example of the results of the tensile test at low and elevated temperatures is shown in **Fig. 15**. Since the tensile strength at room temperature was set at 62 kgf/mm² minimum, it was possible to obtain 55 kgf/mm² at 150°C and 200°C.

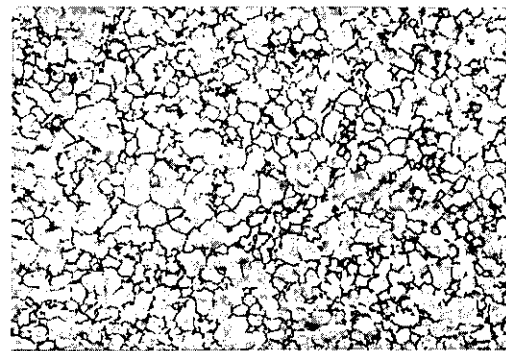
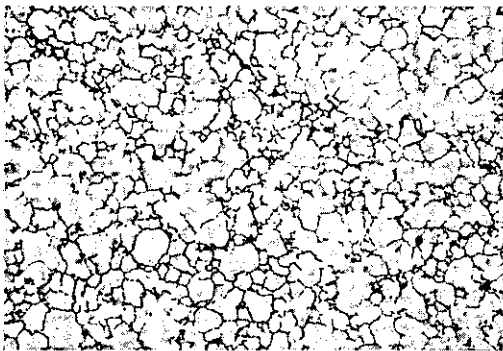
4.4 Impact and Drop-weight Properties

Typical examples of the results of the impact test using a 2 mm V-notch Charpy specimen which was conducted on the top head flange and bottom head dome are shown in **Figs. 13** and **14**, respectively. Since the top head flange had a plate thickness of as

Flange



Dome



Commercial test position

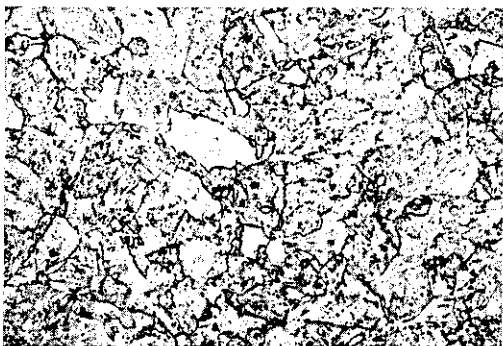
Center($\times 100$)

Photo. 2 Typical austenite grain structures of top head flange and bottom head dome

Flange



Dome



Commercial test position

Center($\times 400$)

Photo. 3 Typical microstructures of top head flange and bottom head dome

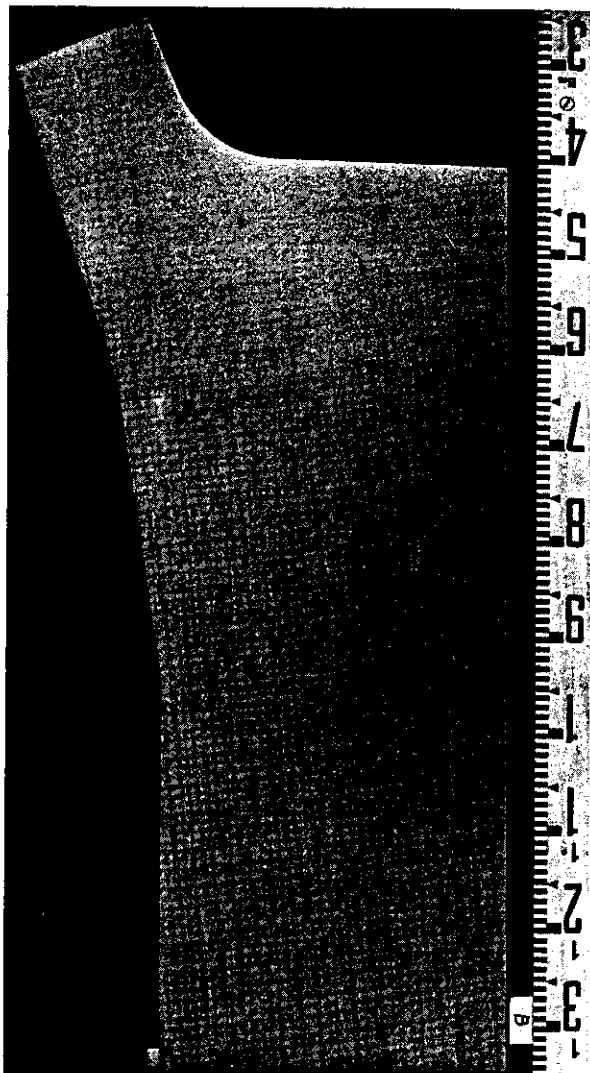


Photo. 4 Typical macro structure of top head flange

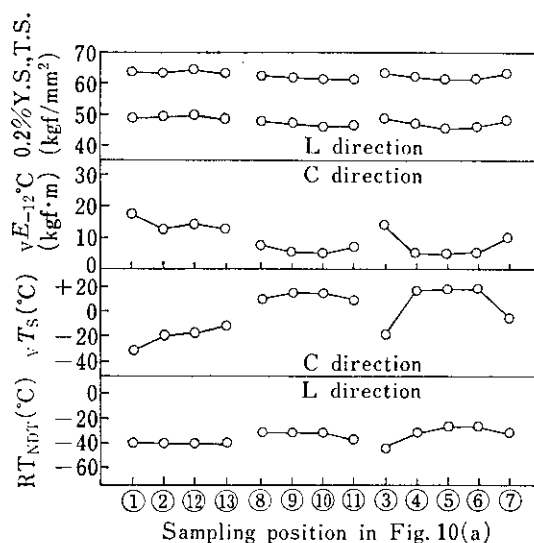


Fig. 13 Distribution of strength and toughness in top head flange

much as about 400 mm, the mass effect was observed, but the circumferential distribution of impact strength was uniform, and the bottom head dome also had uniform circumferential distribution of impact properties, thus indicating that both the products had undergone uniform heat treatment. Typical examples of Charpy transition curves at commercial test positions of the top head flange and bottom head dome

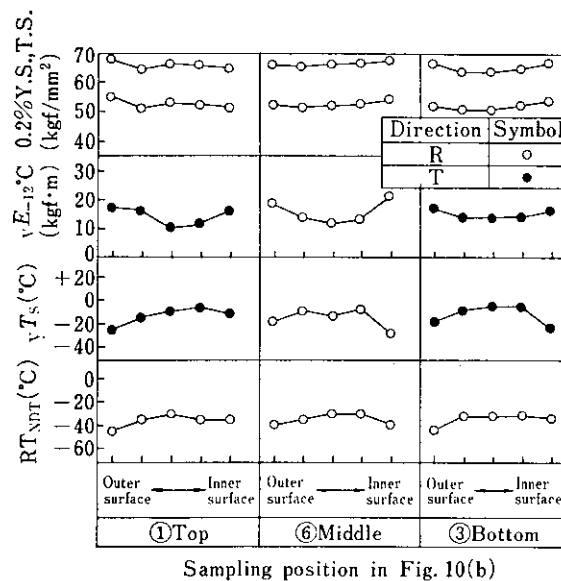


Fig. 14 Distribution of strength and toughness in bottom head dome

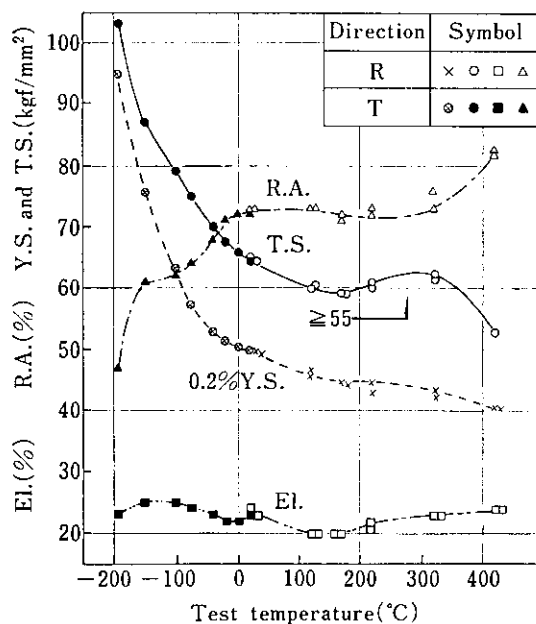


Fig. 15 Influence of test temperature on tensile properties at a quarter thickness of bottom head dome

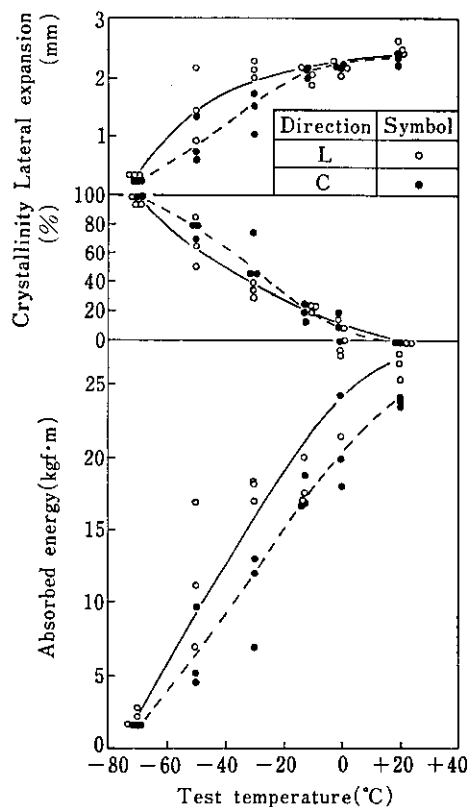


Fig. 16 Charpy transition curve of top head flange at the commercial test position

are shown in Figs. 16 and 17, respectively. The upper shelf energy exceeded 16 kgf·m and was far above the 10.4 kgf·m required by 10 CFR 50 APP.G of NRC of the U.S.

Drop-weight properties were investigated by using ASTM E 208 P-3 type test pieces. Typical examples of test results are shown in Figs. 13 and 14. The T_{NDT} at the central portion of the top head flange was -25°C , and that at the bottom head dome was -30°C . The difference between these two temperatures may be attributable to the difference in cooling rate. The Charpy impact test value and the lateral expansion at a temperature of $T_{NDT} + 33^{\circ}\text{C}$ exceeded 6.9 kgf·m and 0.89 mm respectively at all sampling stations, and it was determined that the T_{NDT} for both products obtained in this test stood for the reference nil-ductility transition temperature (RT_{NDT}) for both the products.

4.5 Fracture Toughness

In order to investigate the fracture toughness of the top head flange and bottom head dome, a three-point bending test (K_{Ic}), instrumental Charpy test (K_{Id}) and compact test (K_{Ia}) were executed. Test results, compared with K_{IR} curve of the ASME

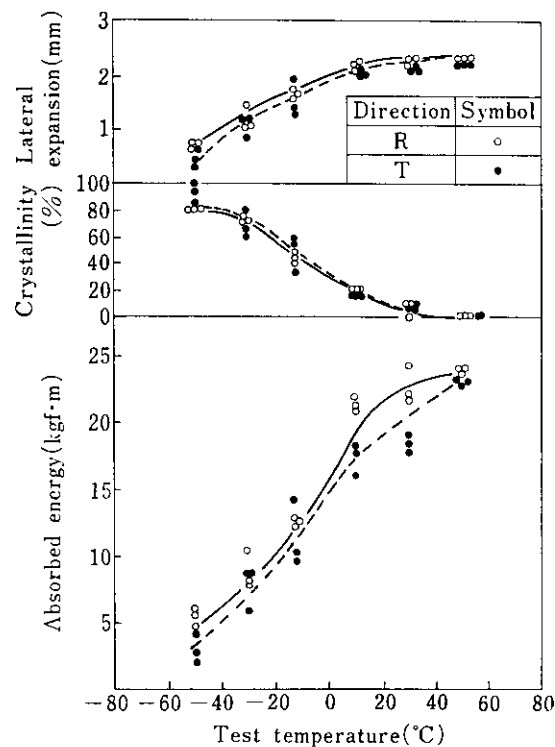


Fig. 17 Charpy transition curve of bottom head dome at 3/4 thickness

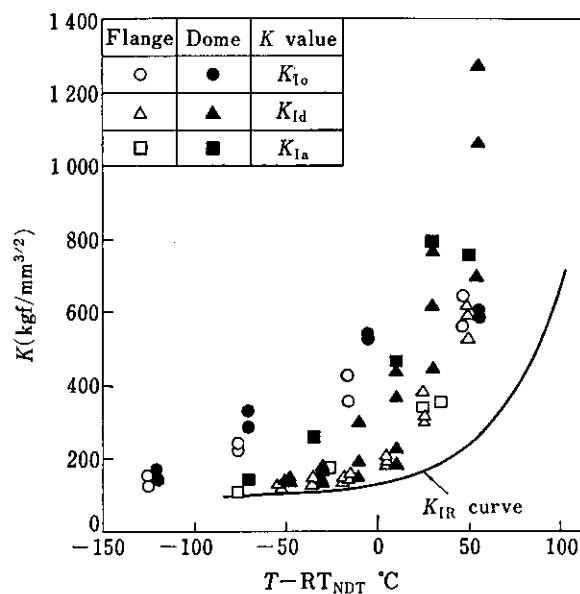


Fig. 18 Temperature dependence of K_{Ic} , K_{Id} and K_{Ia} for top head flange and bottom head dome

Boiler and Pressure Vessel Code Sec. III, are shown in Fig. 18. All the values were above the K_{IR} curve, and it was confirmed that both products had excellent properties against unstable fracture.

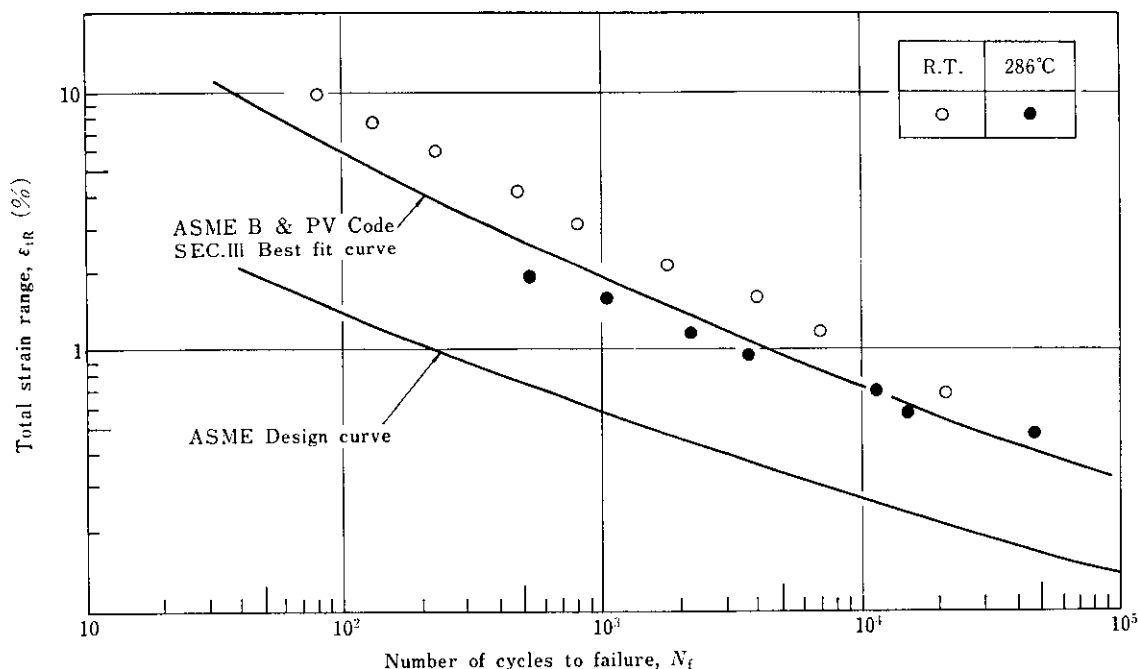


Fig. 19 Results of low cycle fatigue test of bottom head dome at room temperature and at 286°C

4.6 Fatigue Properties

Results of the low-cycle fatigue test at room temperature and elevated temperature (286°C) of the bottom head dome, compared with the design fatigue curve shown in the ASME Boiler and Pressure Vessel Code Sec. III, are shown in Fig. 19. Also, results of the fatigue crack propagation test by the WOL-type of zero tension at room temperature compared with the reference value given by the ASME Boiler and Pressure Vessel Code Sec. XI, are shown in Fig. 20. In the results of the low-cycle fatigue test, the value

at 286°C is on the lower-life side than the value at room temperature, but both these values indicate the same properties as those of the best fit curve, and are on the considerably longer life side than the design curve. The fatigue crack propagation properties are also on the lower side than the reference value, and safety is fully ensured even when an analysis using Sec. XI is to be performed.

5 Discussion

5.1 Mechanical Properties

All the tensile, impact and drop-weight tests gave values that had been originally target. These three properties arranged according to the cooling rate are shown in Fig. 21. This figure indicates that the impact and drop-weight properties, in particular, are greatly dependent upon the cooling rate. In this way, the impact and drop-weight properties are virtually determined by plate thickness during heat treatment. In the present tests, the quality design was mainly based on T.S. at elevated temperature, but as a measure to improve the impact and drop-weight properties, the C content could conceivably be lowered. In such a case, however, guaranteeing both T.S. at room temperature and T.S. at elevated temperature will pose a problem. For this reason, it would be necessary to examine the priority between the two properties, after determining at what point the balance is to be struck between strength and toughness.

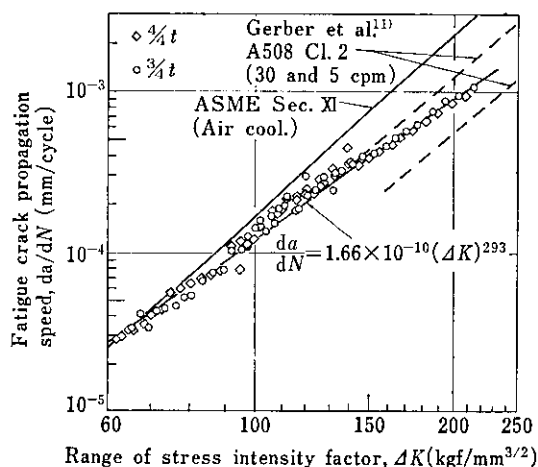


Fig. 20 Relation between fatigue crack propagation speed and range of stress intensity factor of bottom head dome

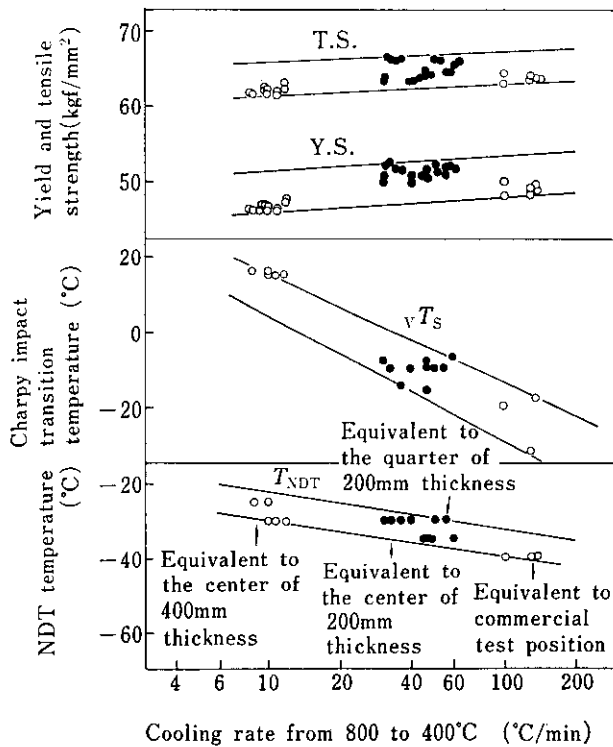


Fig. 21 Effect of cooling rate on tensile properties and toughness of SFVV3 steel

5.2 Flexural Forming Load

Flexural forming load P is obtained as a sum of load P_1 for draw-forming the peripheral portion of the raw material, load P_2 for giving yield flexural forming to the raw material, and friction load P_3 . Symbols required for calculations are given in Fig. 22. Flexural forming load can be obtained by the following equations, if it is assumed in the calculation that ① plate thickness of the raw material will not change during working and ② the raw material is a perfectly rigid plastic body:

$$P_1 = \frac{2.2\pi r_k t \sigma_s \sin \phi}{1 - \cos \phi} \left\{ 1 - \left(\frac{r_0}{r_k} \right)^{1 - \sec \phi} \right\}$$

$$P_2 = \frac{\pi r_k t^2 \sigma_s \cos^2 \phi}{2 \{ r_d - (\rho_p + \rho_d + t) \sin \phi \}}$$

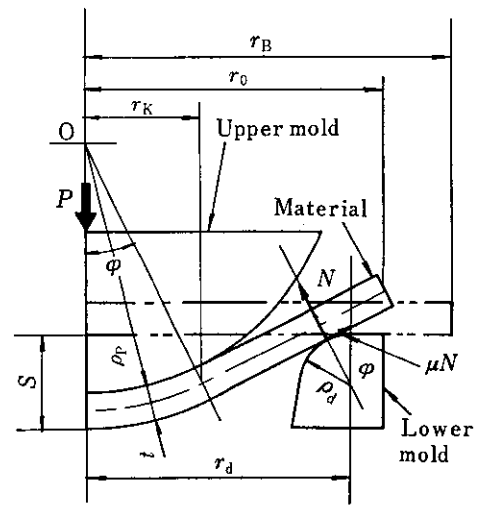
$$P = C(P_1 + P_2)$$

$$P_3 = P - (P_1 + P_2) = (C - 1)(P_1 + P_2)$$

where

$$C = \left[1 - \frac{\mu \rho_d \cos \phi}{(1 + \mu \tan \phi) \{ r_d - (\rho_p + \rho_d + t) \sin \phi \}} \right]^{-1}$$

Forming load for the full-size model calculated by the above equations is the same as that shown earlier in Fig. 4. Major factors that affect the forming load are deformation resistance, plate thickness and the



- P : Forming load
 μ : Friction factor between material and mold
 t : Plate thickness
 ρ_p : Spherical radius of upper mold
 r_B : Radius of blank material
 ϕ : Contact angle of upper mold corresponding to penetration S
 N : Normal reaction of lower mold surface
 S : Penetration of upper mold
 ρ_d : Inside radius of corner area of lower mold
 r_d : Radius of lower mold
 σ_s : Deformation resistance

Fig. 22 Explanation of symbols for calculation

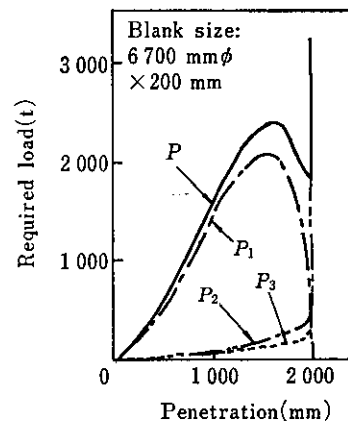


Fig. 23 Calculated change of required forming load and its constituents at 1 000°C with the progress of penetration

diameter of the raw material, mold sizes, and the friction factor at the contact portion between the raw material and mold. The effect of the forming temperature need not be considered directly, if it is taken into

consideration in the form of temperature variation in deformation resistance and in the friction factor. Fig. 23 shows the relationship between forming load and the quantity of penetration according to the former's constituents P_1 , P_2 , and P_3 . The peak point of P is caused by drawing-deformation load P_1 , and the maximum value at the forming completion point is caused by flexural deformation load P_2 . Since P_2 suddenly increases at a point very close to the forming completion point, the diameter of the lower mold should be set slightly larger than the design value in order to be able to complete forming easily with forming load less than the calculated value. Next, the relation between forming load, plate thickness and the blank diameter was calculated. Results of the calculation compensated by actual results are shown in Fig. 24. The relation between forming load and plate thickness is more or less proportional, and the relationship of $P/P_0 \propto 1.02 (t/t_0)$ has been found. To sum up, it is possible to apply flexural forming to the bottom head dome of the 1 100 MWe class with the existing equipment.

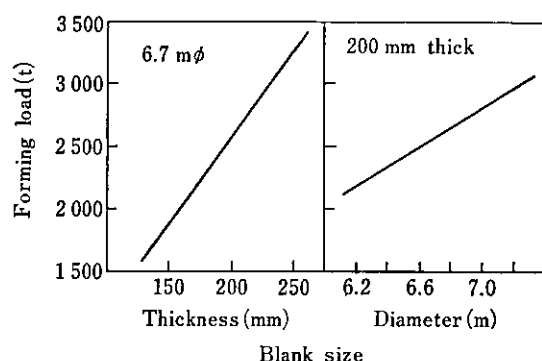


Fig. 24 Required forming load at 1 000°C as a function of blank size

6]Conclusion

The top head flange and bottom head dome for the nuclear pressure vessel were trial-manufactured and their property verification tests conducted. The bottom head dome was given flexural forming with a spherical upper mold and a ring-shaped lower mold, and as a result a dome was obtained with uniform deformation and free of uneven plate thickness and of scale scars which are liable to occur during forming. In the property verification tests, satisfactory values were obtained for internal properties, mechanical properties, fracture toughness and fatigue properties. These trial manufactures and verification tests have paved the way for starting a stable commercial production of forgings for nuclear pressure vessels which fully meet the needs of pressure vessel manufacturers.

References

- 1) K. Emoto, K. Miyata, A. Takahashi, M. Suzuki and T. Sekine: *Kawasaki Steel Technical Report*, 6 (1974) 2, pp. 152-164 (in Japanese)
- 2) T. Nishioka and K. Emoto: *Kawasaki Steel Technical Report*, 4 (1972) 1, pp. 12-24 (in Japanese)
- 3) T. Nishioka and K. Emoto: *Tetsu-to-Hagané*, 60 (1974) 2, 1662
- 4) H. Wanaka, A. Horiuchi, K. Nada, S. Matsui and Y. Hayakawa: *Kawasaki Steel Technical Report*, 8 (1974) 1, pp. 15-28 (in Japanese)
- 5) T. Saito: *Kawasaki Steel Technical Report*, 9 (1977) 3-4, pp. 1-12 (in Japanese)
- 6) S. Sato, T. Enami, Y. Kusuhara and T. Hayashi: *Kawasaki Steel Technical Report*, 4 (1972) 3, pp. 25-55 (in Japanese)
- 7) T. Enami, S. Sato, T. Tanaka and T. Funakoshi: *Kawasaki Steel Technical Report*, 6 (1974) 2, pp. 15-31 (in Japanese)
- 8) T. Enami, T. Hatomura, T. Tanaka, T. Funakoshi: *Kawasaki Steel Technical Report*, 6 (1974) 2, pp. 32-43 (in Japanese)
- 9) Y. Kusuhara, S. Yoshimura, Y. Ogino, T. Enami, T. Funakoshi and T. Hayashi: *Kawasaki Steel Technical Report*, 6 (1974) 2, pp. 44-68 (in Japanese)
- 10) T. Hiro, N. Nishiyama, J. Tsuboi, R. Okabe and T. Mori: *Kawasaki Steel Technical Report*, 6 (1974) 2, pp. 69-86 (in Japanese)
- 11) T.L. Gerber, J.D. Heald, and E. Kiss: *J. Eng. Mat. Technol., Trans. ASME*, (1974), p. 255